UC Irvine
UC Irvine Previously Published Works

Title

Organo-functionalized metal–oxide clusters: synthesis and characterization of the reduced cationic species [NaV IV 6 O 6 {(OCH 2 CH 2) 2 NH} 6] +

Permalink

Journal

Dalton Transactions, 43(43)

ISSN

1477-9226

Authors

Khan, M Ishaque
Zheng, Y
Li, H
et al.

Publication Date

2014-11-21

DOI

10.1039/c4dt02174f

Copyright Information

Peer reviewed

PAPER

CrossMark
click for updates

Organo-functionalized metal–oxide clusters: synthesis and characterization of the reduced cationic species [NaV$^{IV}_6$O$_6${(OCH$_2$CH$_2$)$_2$NH}$_6$]$^+$†

M. Ishaque Khan,*[a] Y. Zheng,[a] H. Li,[a] L. Swenson,[a] A. Basha[a] and R. J. Doedens[b]

A new heteropolyoxovanadium compound, [NaV$_6$O$_6${(OCH$_2$CH$_2$)$_2$NH}$_6$]·(OH)$_{0.5}$Cl$_{0.5}$·3(H$_2$O), was synthesized and characterized by single-crystal X-ray diffraction analysis, cyclic voltammetry, FTIR and UV-vis spectroscopy, and TGA. [NaV$_6$O$_6${(OCH$_2$CH$_2$)$_2$NH}$_6$]·(OH)$_{0.5}$Cl$_{0.5}$·3(H$_2$O) contains the diethanolamine functionalized oxovanadium cationic cluster, [NaV$^{IV}_6$O$_6${(OCH$_2$CH$_2$)$_2$NH}$_6$]$^+$. The cluster cation is composed of a fully reduced cyclic {NaV$_6$N$_6$O$_{18}$} framework which adopts an Anderson-like structure and is comprised of a ring of six edge-sharing {VO$_5$N} octahedra linked to a central {NaO$_6$} unit. Two (OCH$_2$CH$_2$–) arms of each of the six diethanolamine ligands are incorporated into the oxometalate core. FTIR spectra are consistent with the presence of expected V=O$_t$ stretching modes and functionalization with diethanolamine. Electrochemical and UV-vis absorption properties are consistent with two distinct MLCT processes: the characteristic V=O$_t$ dπ–pπ interaction, and a second process occurring through the hydrogen-terminated nitrogen atoms (V–N–H) of the octahedra forming the cyclic {NaV$_6$N$_6$O$_{18}$} core.

Introduction

Polyoxometalates (POMs) are polynuclear, metal–oxide anionic clusters formed mainly by the early transition metals V, Mo, and W, usually in their highest (d^0) oxidation state.[1,2] POMs have (idealized) symmetric structures composed of metal–oxygen polyhedra joined by corner- and edge-sharing of oxygen atoms. A number of prototypical POM structures are common, for example the Lindqvist (M$_6$O$_{19}$), Anderson (XM$_6$O$_{24}$), Keggin (XM$_{12}$O$_{40}$), and Dawson (X$_2$M$_{18}$O$_{62}$) structures.[1,2] Double-bonded, non-bridging oxygen atoms (M=O$_t$) terminate at the anion surface and offer a more-or-less facile dπ–pπ electron transfer path to the metal atoms, which may be reduced thereby to obtain mixed valence (d^0/d^1) POM anions. A general redox capacity results from this interaction and is the origin of the compelling electronic and photophysical properties that are generally exhibited by POM anions. Broadly considered, these are the ability to accept multiple electrons in a chemically reversible manner,[2] and the presence of characteristic near-UV oxygen-to-metal (M=O$_t$) charge-transfer bands.[2] Their practical application is found, for example, in oxidative chemical[3–5] and photochemical[6–8] catalysis. Reduced POMs

support unpaired electrons and are thus attractive as potential magnetic centers.[9,10] POMs may be functionalized by replacement of some portion of the metal–oxygen framework by another atomic or molecular species, modifying their chemical properties and facilitating incorporation into extended structures.[11,12] This has led to the introduction of a variety of functionalized POM types and to a diversity of POM organic framework (POMOF) materials in which POM units are linked into chains, sheets, and 3D structures.[13–15]

Of the prototypical POM structures, not all are observed for even the most common POM-forming elements (V, Mo, and W). For example, there is no vanadium analogue of the Lindqvist and Anderson[16] structures formed from molybdenum. POMs are derived from mono- and polynuclear metal oxide precursors by bench top and solvothermal methods. Covalent POM functionalization is often realized by self-assembly through addition of organic ligands to POM precursors.[11,12] The ligands are integrated into the metal oxide framework through (usually) a terminal oxygen atom (e.g. the hydroxyl oxygen of an alkoxide). Covalently functionalized polyoxovanadates began to appear apace around 25 years ago, and a number of early contributions[17] demonstrated the accessibility of functionalized polyoxovanadates containing the Lindqvist (e.g., [V$_6$O$_{13}${O$_2$NC(CH$_2$O)$_3$}$_2$]$^{2-}$)[18] and Anderson (e.g. [(VO)$_6$(CO$_3$)$_4$(OH)$_9$]$^{5-}$)[19] structures.

As part of a continuing effort to synthesize new functionalized polyoxovanadate species with interesting electronic and magnetic properties, we prepared a series of new organo-functionalized heteropolyoxovanadium(IV) POMs,[20,21] of which

[a]Department of Biological and Chemical Sciences, Illinois Institute of Technology, Chicago, IL 60616, USA. E-mail: khan@iit.edu
[b]Department of Chemistry, University of California, Irvine, CA 92697, USA

$[NaV^{IV}_6O_6\{(OCH_2CH_2)_2N(CH_2CH_2OH)\}_6]Cl \cdot H_2O$ (**C1**) is a prototypical example. Compound **C1** was prepared by a solvothermal reaction of triethanolamine $\{N(CH_2CH_2OH)_3\}$ and ammonium decavanadate $\{(NH_4)_6[V_{10}O_{28}] \cdot 6H_2O\}$.[21] **C1** is composed of a cyclic $\{NaV_6N_6O_{18}\}$ framework decorated with six triethanolamine ligands forming the cationic cluster $[NaV^{IV}_6O_6\{(OCH_2CH_2)_2N(CH_2CH_2OH)\}_6]^+$ (Fig. 1a); a chloride anion balance charge. The previously unobserved $\{NaV_6N_6O_{18}\}$ core adopts an Anderson-like[16] structure and is comprised of a ring of six edge-sharing $\{VO_5N\}$ octahedra linked to a central $\{NaO_6\}$ unit. Two (OCH_2CH_2-) arms of each of the six triethanolamine ligands are incorporated into the oxometalate core, the third $\{-CH_2CH_2OH\}$ arm remains pendant. The hexametalate ring contains six d^1 (V^{IV}) ions and variable temperature magnetic susceptibility measurements indicate ferromagnetic interactions of the six d^1 spin centers below room temperature.[21]
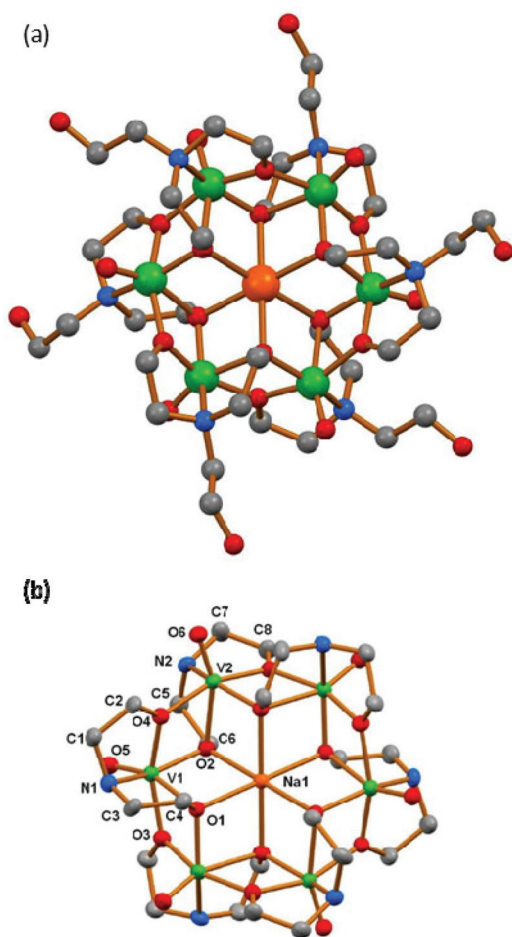

Fig. 1 Ball-and-stick views of the cationic cores of (a) $[NaV^{IV}_6O_6\{(OCH_2CH_2)_2N(CH_2CH_2OH)\}_6]^+$ (**C1**) and (b) $[NaV^{IV}_6O_6\{(OCH_2CH_2)_2NH\}_6]^+$ (**C3**). The **C1** core is identical to the **C3** core except that the six ethanolic pendant arms of **C1** are replaced by hydrogen atoms (not shown in the figure) in **C3**. Color key: sodium (orange), vanadium (green), oxygen (red), nitrogen (blue), carbon (grey). Hydrogen atoms are omitted for clarity.

Substitution of the ligand, *N,N*-bis(2-hydroxyethyl)ethylenediamine $\{(HOCH_2CH_2)_2NCH_2CH_2NH_2\}$ (**L**), for triethanolamine in the reaction forming **C1** yielded the compound $[NaV^{IV}_6O_6\{(OCH_2CH_2)_2NH\}_6](OH)_{0.5} \cdot Cl_{0.5} \cdot (HOCH_2CH_2)_2N(CH_2CH_2NH_2)$ (**C2**). Although the structure of **C2** was poorly resolved, it was clear that it contained the cationic cluster $[NaV^{IV}_6O_6\{(OCH_2CH_2)_2NH\}_6]^+$ with the same $\{NaV_6N_6O_{18}\}$ metallacyclic core observed in **C1**, but with six $\{HN(CH_2CH_2OH)_2\}$ ligands, and no pendant $\{-CH_2CH_2NH_2\}$ arms, as shown for the closely related compound **C3** in Fig. 1b. The functionalization of the oxometallic $\{NaV_6O_6\}$ core with diethanolamine ligands in **C2** indicates that some of the ligand **L** has undergone bond cleavage of the $\{CH_2CH_2NH_2\}$ group with concomitant protonation of nitrogen during the formation of **C2**. Interestingly, some of the uncleaved **L** is also present as a free molecule in the crystals of **C2**. The diethanolamine-functionalized cationic core of **C2** offers the compelling prospect of versatile chemical activity at the NH groups, conceivably leading to a diversity of secondary functionalization. We therefore undertook to synthesize a compound containing the cationic core of **C2** by a direct method using diethanolamine $(CH_2CH_2OH)_2NH$. Here we report the successful synthesis of the title compound, $[NaV_6O_6\{(OCH_2CH_2)_2NH\}_6] \cdot (OH)_{0.5}Cl_{0.5} \cdot 3(H_2O)$ (**C3**), directly from the solvothermal reaction of the diethanolamine ligand and ammonium decavanadate $(NH_4)_6[V_{10}O_{28}] \cdot 6H_2O$.

Experimental

Materials and methods

Commercially available reagent-grade chemicals were obtained from Sigma-Aldrich and used without additional purification. Ammonium decavanadate $\{(NH_4)_6[V_{10}O_{28}] \cdot 6H_2O\}$ was synthesized according to a literature method.[22] $[NaV^{IV}_6O_6\{(OCH_2CH_2)_2N(CH_2CH_2OH)\}_6]Cl \cdot H_2O$ (**C1**) was synthesized as previously reported.[21] All CV experiments were carried out using a BASi Epsilon potentiostat in a three-electrode cell using a 3 mm diameter glassy carbon working electrode, a Ag/AgCl reference electrode, and a platinum wire counter electrode. The electrolyte was 0.01 M NaCl. The glassy carbon working electrode was polished (1 μm) prior to obtaining each CV and the corresponding background. Potentials are reported *versus* the normal hydrogen electrode. FTIR spectra were obtained (4000–400 cm^{-1}, KBr method) using a Thermo Nicolet NEXUS 470 FT-IR spectrometer and processed using the Thermo Fisher Scientific OMNIC v8.3 software. TGA curves were obtained at 3 °C min^{-1} in argon (100 SCCM) using a Mettler Toledo TGA/SDTA 851e and processed using the STARe v10.00 software. UV-vis spectra (190–800 nm, quartz cuvette, 1 cm path length) of 1×10^{-4} M solutions of **C1** and **C3** were obtained using a Beckman Coulter DU 800 UV/vis spectrophotometer and processed using the Beckman Coulter DU 800 System and Applications software v2.1.

Synthesis of $\{NaV^{IV}_6O_6[(OCH_2CH_2)_2NH]_6\}(OH)_{0.5} \cdot Cl_{0.5} \cdot (HOCH_2CH_2)_2N(CH_2CH_2NH_2)$ (**C2**). In a typical synthesis,

0.0684 mmol $[NH_4]_6[V_{10}O_{28}]\cdot 6H_2O$, 0.17 mmol NaCl, and 2.38 mmol $(HOCH_2CH_2)_2NCH_2CH_2NH_2$ were mixed together and placed in a 23 ml Teflon-lined Parr autoclave. The reactor was heated in a Thermoline furnace at 145 °C for 24 h. The reaction vessel was then allowed to cool to room temperature over a period of 72–96 h. The resulting product, a blue crystalline material, was transferred to filter paper and rapidly washed with three 3 ml portions of CH_3CN. The crystalline material was then dried under ambient conditions to give $\{NaV^{IV}_6O_6[(OCH_2CH_2)_2NH]_6\}(OH)_{0.5}\cdot Cl_{0.5}\cdot(HOCH_2CH_2)_2N(CH_2CH_2NH_2)$ (**C2**) in ~20% (based on vanadium) yield (Found: Na, 1.91; V, 22.09; C, 29.58; H, 6.23; N, 9.48; Cl, 0.90. Calc. for **C2**: Na, 1.89; V, 25.10; C, 29.58; H, 5.85; N, 9.2; Cl, 1.46). The crystalline product was soluble in CH_3CN and could be recrystallized by evaporative crystallization from 20 to 25 ml of CH_3CN to obtain crystals suitable for single crystal XRD.

Synthesis of $[NaV_6O_6\{(OCH_2CH_2)_2NH\}_6]\cdot(OH)_{0.5}Cl_{0.5}\cdot 3(H_2O)$ (C3). In a typical synthesis, ammonium decavanadate $[NH_4]_6V_{10}O_{28}\cdot 6H_2O$ (0.0684 mmol) was combined with NaCl (0.17 mmol) and diethanolamine $\{(CH_2CH_2OH)_2NH\}$ (2.37 mmol) in a 23 ml Teflon-lined Parr reaction vessel and heated at 145 °C for 24 hours. The vessel was allowed to stand for a further 24 hours at 25 °C. The reaction yielded a two phase product composed of a dark blue solid surrounded by a blue gelatinous liquid. The two phases were dissolved together in water. The solution was allowed to evaporate slowly at room temperature to produce dark blue crystals of the final product, $[NaV_6O_6\{(OCH_2CH_2)_2NH\}_6]\cdot(OH)_{0.5}Cl_{0.5}\cdot 3(H_2O)$ in ~55% yield (based on V). (Found: C, 25.7; N, 7.3; H, 5.1; Cl, 1.7. Calc. for **C3**: C, 25.65; N, 7.5; H, 5.4; Cl, 1.6%.) The calculated values are based on the X-ray results, with the addition of disordered fractional Cl^- and OH^- ions to conform to the elemental analysis and to provide charge balance.

Single crystal X-ray structure analysis

An X-ray quality crystal of **C3** (blue plate, 0.25 × 0.22 × 0.10 mm³) was mounted on a thin glass fiber with hydrocarbon oil. A full sphere of data was collected at −185 °C on a Bruker SMART APEX II diffractometer equipped with graphite monochromatized Mo Kα radiation. The data were processed with the SAINT software[23] and corrected for absorption with SADABS.[24] Calculations were performed by the use of the SHELXTL package.[25] Hydrogen atoms, except for those on a disordered water oxygen atom, were located and refined by the use of the riding model. At this point, the difference map was featureless and the unit cell had large void areas with an unrealistic volume of 26.5 Å³ per non-hydrogen atom. Also, the calculated value of 1.18 g cm⁻³ for the density was inconsistent with the observed density of 1.67 g cm⁻³. The PLATON/SQUEEZE program[26] was used to model the electron density in the void areas. The color diagrams were produced using Mercury and POV-ray. Further details are included in the deposited .cif file. The Crystallographic information file (CIF) is available at the Cambridge Crystallographic Data Center (CCDC 994749).[27]

Results and discussion

Synthesis

We obtained the title compound, $[NaV_6O_6\{(OCH_2CH_2)_2NH\}_6]\cdot(OH)_{0.5}Cl_{0.5}\cdot 3(H_2O)$ (**C3**), directly from the solvothermal reaction of diethanolamine, sodium chloride and ammonium decavanadate without using a formal solvent. While **C1** was obtained in the presence of a mixed acetonitrile–ethanol solvent, we could not obtain **C3** in either acetonitrile or ethanol, or an acetonitrile–ethanol mixture. This suggests that diethanolamine, unlike triethanolamine, interacts sufficiently with acetonitrile and ethanol to inhibit its reaction with the vanadium oxide intermediates present in the reaction vessel under solvothermal conditions. TGA indicated that the as-synthesized material contained about 4.5 weight percent water which was removed at a low temperature ($T < 100$ °C). No weight loss associated with organic material was observed until $T > 200$ °C (under Ar, see ESI†), indicating that the organo-functionalized core has good thermal stability.

Crystal structure

Compound **C3** is a new organo-functionalized heteropolyoxovanadium(IV) compound. Its structure, revealed by single crystal X-ray structure analysis, contains the novel cation cluster species $[NaV^{IV}_6O_6\{(OCH_2CH_2)_2NH\}_6]^+$ (Fig. 1b). Its structure consists of a fully reduced cyclic $\{NaV_6N_6O_{18}\}$ framework incorporating six diethanolamine ligands, chloride and hydroxide anion balance charge. The $\{NaV_6N_6O_{18}\}$ core adopts an Anderson-like structure[16] comprising of six edge-sharing distorted $\{VO_5N\}$ octahedra linked to the central $\{NaO_6\}$ unit. The octahedral geometry around each vanadium atom of the cyclic core is defined by five atoms from the diethanolamine ligands and one terminal oxygen atom ($V=O_t$). The $\{V_6O_{12}\}$ ring in **C3** may be regarded as a hexadentate ligand to the metal Na, forming a $\{NaV_6O_{12}\}$ chelate. Like **C1**, the hexametalate ring of **C3** contains six d^1 (V^{IV}) ions.

The two crystallographically independent vanadium atoms have virtually identical distorted octahedral configurations with bond distances in the expected ranges (mean values include V–N = 2.170(3) Å; V–μ¹O = 1.618(2) Å; V–μ²O = 1.995(2) Å; V–μ³O = 2.109(2) Å; Na1–O = 2.300(3) Å). Full details of the structural analysis, including tables of distances and angles, are included in the deposited cif file.

FTIR spectroscopy

The characteristic polyoxoanion FTIR spectrum contains a strong band associated with a $M=O_t$ vibrational mode and a number of lower energy bands associated with the vibrational modes of bridging oxygen atoms. The prototypical Anderson structure[16] is mainly observed as a polyoxomolybdate species $\{(XMo_6O_{24})\}$ and we could find no polyoxovanadate examples in the literature. A variety of different salts of this species have been characterized using FTIR and Raman spectroscopy methods and certain main vibrational modes have been assigned.[28–31] The Anderson structure contains two equivalent terminal molybdenum–oxygen bonds ($Mo=O_t$) which typically

show strong IR absorption bands around 950 (ν_{sym}Mo=O_t) and 890 cm^{-1} (ν_{as}Mo=O_t). The structures of **C1** and **C3**, while conceptually derived from the Anderson structure, are expected to exhibit significant deviations from the prototypical Anderson FTIR spectrum due to the organo-functionalization, where one terminal oxygen per vanadium addendum atom has been replaced by the nitrogen atom of the triethanolamine (**C1**) and diethanolamine (**C3**) ligands, and all remaining non-terminal surface oxygen atoms are bound to the organo carbon atoms. The terminal oxygen atoms (V=O_t) remain as a basic structural similarity between the prototypical Anderson structure and the structures of both **C1** and **C3**. Therefore we might expect some commonality in the FTIR spectra of each species in regard to the terminal oxygen (M=O_t). And indeed, each of the **C1** and **C3** spectra contains a feature centered around 950 cm^{-1} that appears to be a composite of two bands (Fig. 2a). We assign one of these bands to the (ν_{sym}V=O_t) mode of **C1** and **C3** in comparison with the prototypical

(ν_{sym}Mo=O_t) band, and consider the possibility that the remaining band is associated with a V–N mode (*e.g.*, ν_{sym}V–N). The proximity of these features in the **C1** and **C3** spectra implies that the asymmetric stretch associated with the terminal oxygen atom (ν_{as}V=O_t) should also be closely located in each spectra, and indeed a common feature is observed in both spectra at ~881 cm^{-1}. The remaining bands below 950 cm^{-1} are not inconsistent with contributions due to the ethanolamine functionalization[32] and various expected V–O–V vibrational modes. The multiple bands in the ~1500–1000 cm^{-1} region of the **C1** and **C3** FTIR spectra are also consistent with the respective organic ligands.[32] The C–H stretching vibrations of normal alkanes appear in the 3000–2840 cm^{-1} region (Fig. 2b). Four peaks associated with the asymmetric and symmetric C–H stretching modes of the methyl and methylene groups are usually observed. For example, in dodecane, $\nu_{as}CH_3 = 2962$, $\nu_s CH_3 = 2872$, $\nu_{as}CH_2 = 2926$, and $\nu_s CH_2 = 2853$ cm^{-1}.[33] We attribute the multiple features observed in the 3000–2840 cm^{-1} region of the **C1** and **C3** FTIR spectra to non-equivalent methylene groups contained in the organic ligands of **C1** and **C3**. A broad O–H stretching band appears in the 3700–3000 cm^{-1} region due to the presence of surface water and water of crystallization contained in the polycrystalline powder samples of both **C1** and **C3**. The **C3** spectrum contains an additional band superimposed on the broad O–H stretching band and centered at 3235 cm^{-1}. Primary amines display asymmetrical and symmetrical N–H stretching modes around 3500 and 3400 cm^{-1}, respectively. Secondary amines display a single band around 3330 cm^{-1} (*e.g.* diethanolamine, 3288). No bands are present above the aliphatic C–H stretching region (*i.e.* >3000 cm^{-1}) in tertiary amines (*e.g.* triethanolamine).[33] We therefore attribute the 3235 cm^{-1} band of the FTIR spectrum of **C3** to the N–H stretching mode associated with its diethanolamine functionalization.
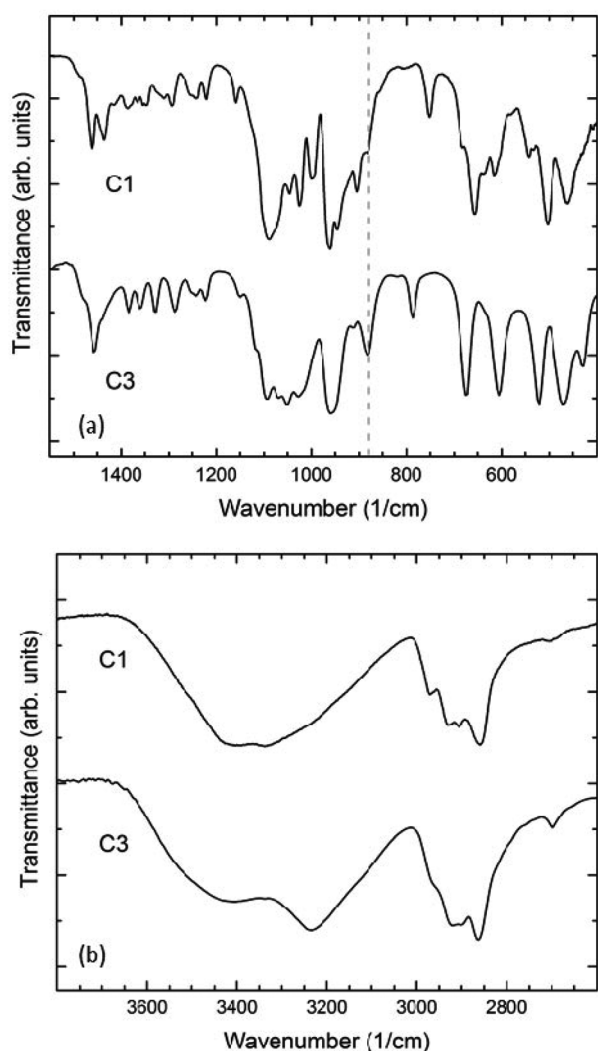
Cyclic voltammetry

We investigated the aqueous phase electrochemical redox properties of the title compound and **C1** by cyclic voltammetry (CV). Unfunctionalized POMs exhibit CV reduction waves in accord with the high oxidation state of the metal atoms—usually d^0 or a mixed valence combination of d^0 and d^1. Electrochemical reduction is accompanied by electron transfer from terminal (non-bridging) oxygen surface atoms to the d^0 polyhedral metal atoms through the M=O_t dπ–pπ interaction.[1] The functionalized POMs **C1** and **C3** could not be electrochemically reduced, but each exhibited a chemically irreversible oxidation wave (Fig. 3). This result is in accord with the fully reduced (d^1) state of each compound, which energetically disfavors further reduction. Electrochemical oxidation is accompanied by electron transfer from the d^1 vanadium (V^{IV}) to the terminal oxygen surface atom. This irreversible nature of the CV profile suggests decomposition of the cationic core upon oxidation. This behavior may be contrasted with, for example, the fully oxidized Lindqvist hexavanadate, $[V^V_6O_{13}\{O_2NC(CH_2O)_3\}_2]^{2-}$, which displays a reversible one-electron reduction.[34] Peak positions indicate that **C3** is more

Fig. 2 FTIR spectra of [NaV$^{IV}_6$O$_6${(OCH$_2$CH$_2$)$_2$N(CH$_2$CH$_2$OH)}$_6$]Cl·H$_2$O (**C1**) and [NaV$_6$O$_6${(OCH$_2$CH$_2$)$_2$NH}$_6$]·(OH)$_{0.5}$Cl$_{0.5}$·3(H$_2$O) (**C3**) in the (a) 1550–400 and (b) 3800–3200 cm^{-1} region. The dashed line of (a) indicates the proposed ν_{as}V=O_t band position.
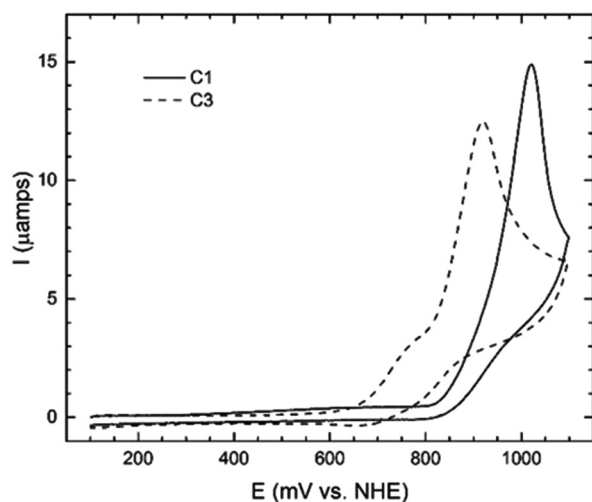
Fig. 3 Background subtracted cyclic voltammograms (200 mV s^{-1}) of aqueous **C1** and **C3** (4×10^{-4} M) obtained in 0.01 M NaCl on a glassy carbon electrode.

easily oxidized than **C1**, a result that may be rationalized on the basis of an effectively larger interfacial charge transfer distance expected for **C1** due to the presence of the pendant ethanolic $\{-CH_2-CH_2-OH\}$ arms.[35] A leading shoulder is present in the CV profile of **C3**. Scan-rate dependent CV excluded adsorption of the oxidized species as the cause of the leading shoulder.[35] We suspect that this shoulder originates in a V–N orbital interaction that allows electron transfer from the d^1 metal to the nitrogen atom, analogous to the dπ–pπ interaction centered on the V=O$_t$ double bond. Thus we suggest that **C3** can be oxidized at nitrogen with an accompanying vanadium-to-nitrogen electron transfer. The absence of a corresponding shoulder in the CV of **C1** (Fig. 3) may be rationalized by insufficient overlap of electrodic and molecular orbitals (centered on nitrogen) due to the presence of the pendant ethanolic arms of **C1** (Fig. 1).

UV-vis spectroscopy

Aqueous phase UV-vis spectra of **C1** and **C3** indicate a strong UV charge transfer band peaking around 200 nm (Fig. 4). Such bands are typical of unfunctionalized POMs and are associated with the same oxygen-to-metal electron transfer that accompanies electrochemical reduction.[2] The fully reduced state (d^1) of the functionalized POM cations of **C1** and **C3**, along with the oxidation wave indicated in the CV, imply that the CT bands of Fig. 4 are associated with oxidative vanadium-to-oxygen charge transfer. A leading, albeit weak, near-UV shoulder is present in both spectra (Fig. 4 inset), indicating that an additional charge transfer process is present, in support of the proposed V–N CT orbital interaction.

Conclusions

We have introduced a new heteropolyoxovanadium compound, $[NaV_6O_6\{(OCH_2CH_2)_2NH\}_6]\cdot(OH)_{0.5}Cl_{0.5}\cdot3(H_2O)$ (**C3**), contain-
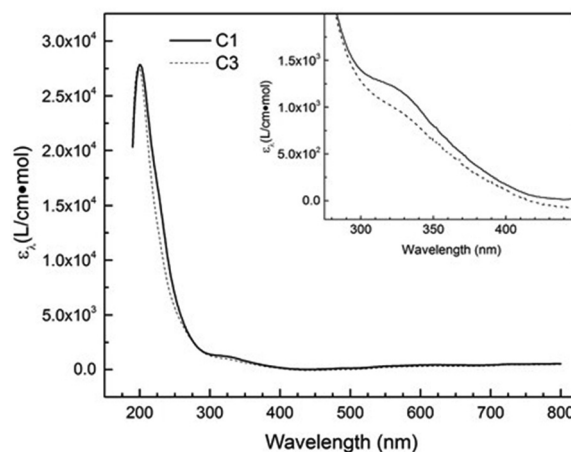

Fig. 4 UV-vis absorption spectra of aqueous **C1** and **C3**. Both species exhibit a strong charge transfer band ($\varepsilon_{max} \sim 200$ nm) having a weak leading shoulder (inset).

ing the diethanolamine functionalized oxovanadium cationic cluster, $[NaV^{IV}_6O_6\{(OCH_2CH_2)_2NH\}_6]^+$. The cluster cation is composed of a fully reduced cyclic $\{NaV_6N_6O_{18}\}$ framework which adopts an Anderson-like structure. **C3** can be obtained in a direct solvothermal reaction of diethanolamine and ammonium decavanadate without any formal solvent present. Electrochemical and UV-vis absorption properties of **C3** are consistent with two distinct MLCT processes: the characteristic V=O$_t$ dπ–pπ interaction, and a second process occurring through the hydrogen-terminated nitrogen atoms (V–N–H) of the octahedra forming the cyclic $\{NaV_6N_6O_{18}\}$ core. This view of the V–N bond as an oxidation route suggests possible chemical activity of the title compound at the hydrogen-terminated nitrogen atoms, and is under further investigation in our laboratory.

Notes and references

1 Special thematic issue on polyoxometalates. Hill, C. L. (Guest Ed.), *Chem. Rev.*, 1998, **98**, 1–390.
2 M. T. Pope, *Heteropoly and Isopoly Oxometalates*, Springer Verlag, West Berlin, 1983.
3 I. V. Kozhevnikov, *Chem. Rev.*, 1998, **98**, 171–198.
4 N. Mizuno and M. Misono, *Chem. Rev.*, 1998, **98**, 199–218.
5 I. A. Weinstock, *Chem. Rev.*, 1998, **98**, 113–170.
6 G. Marci, E. I. Garcia-Lopez and L. Palmisano, *Eur. J. Inorg. Chem.*, 2014, 21–35.
7 E. Papaconstantinou, *Chem. Soc. Rev.*, 1989, **18**, 1–31.
8 E. Papaconstantinou and A. Hiskia, Photochemistry and Photocatalysis by Polyoxometalates, in *Polyoxometalate Molecular Science*, ed. J. J. Borrás-Almenar, E. Coronado, A. Müller and M. Pope, Springer, Netherlands, 2003, pp. 381–416.
9 J. M. Clemente-Juan and E. Coronado, *Coord. Chem. Rev.*, 1999, **193–195**, 361–394.

10 A. Müller, F. Peters, M. T. Pope and D. Gatteschi, *Chem. Rev.*, 1998, **98**, 239–272.

11 A. Proust, B. Matt, R. Villanneau, G. Guillemot, P. Gouzerh and G. Izzet, *Chem. Soc. Rev.*, 2012, **41**, 7605–7622.

12 A. Proust, R. Thouvenot and P. Gouzerh, *Chem. Commun.*, 2008, 1837–1852.

13 M. I. Khan and L. Swenson, Open-Framework Hybrid Materials and Composites from Polyoxometalates, in *New and Future Developments in Catalysis: Hybrid Materials, Composites, and Organocatalysts*, ed. S. Suib, Elsevier, Amsterdam, 2013, pp. 27–54.

14 B. Nohra, H. El Moll, L. M. Rodriguez Albelo, P. Mialane, J. Marrot, C. Mellot-Draznieks, M. O'Keeffe, R. Ngo Biboum, J. Lemaire, B. Keita, L. Nadjo and A. Dolbecq, *J. Am. Chem. Soc.*, 2011, **133**, 13363–13374.

15 Y. F. Song, D. L. Long, C. Ritchie and L. Cronin, *Chem. Rec.*, 2011, **11**, 158–171.

16 J. S. Anderson, *Nature*, 1937, **140**, 850–850.

17 For an early review emphasizing ligand types, synthetic methodologies, and structural characteristics, see: M. I. Khan and J. Zubieta, Oxovanadium and Oxomolybdenum Clusters and Solids Incorporating Oxygen-Donor Ligands, in *Progress in Inorganic Chemistry*, ed. K. D. Karlin, John Wiley & Sons, New York, 1995, vol. 43, pp. 1–149.

18 Q. Chen and J. Zubieta, *Inorg. Chem.*, 1990, **29**, 1456–1458.

19 T. C. W. Mak, P. Li, C. Zheng and K. Huang, *J. Chem. Soc., Chem. Commun.*, 1986, 1597–1598.

20 M. I. Khan, S. Tabussum and R. J. Doedens, *Chem. Commun.*, 2003, 532–533.

21 M. I. Khan, S. Tabussum, R. J. Doedens, V. O. Golub and C. J. O'Connor, *Inorg. Chem.*, 2004, **43**, 5850–5859.

22 W. G. Klemperer, *Inorg. Synth.*, 1990, **27**, 71–85.

23 *SAINT, Version 7.68A*, Bruker-AXS, Madison, WI, 2009.

24 G. M. Sheldrick, *SADABS, Version 2008/1*. University of Göttingen, Germany, 2008.

25 *SHELXTL Version 2008/3*, Bruker-AXS, Madison, WI.

26 A. L. Spek, *PLATON/SQUEEZE*, University of Utrecht, 2011.

27 Crystal data for $C_{16}H_{36}N_4Na_{0.67}O_{14}V_4$: M = 727.6 g mol^{-1}, cubic, space group $P2_13$, a = 18.316(2) Å, V = 6144(2) Å^3, Z = 6, T = 88(2) K, ρ_{calc} = 1.180 Mg m^{-3}, $F(000)$ = 2228, μ(MoKα) = 0.939 mm^{-1}, R_{int} for 74 709 data collected = 0.0446. For refinement of 179 parameters based on 5107 independent data R_1 = 0.0484 (all data), wR_2 = 0.1408, S = 1.125. 2θ(max) = 56.6°. Full details are included in the deposited .cif file, available from the Cambridge Crystallographic Data Center (CCDC 994749).

28 C. Martin, C. Lamonier, M. Fournier, O. Mentré, V. Harlé, D. Guillaume and E. Payen, *Inorg. Chem.*, 2004, **43**, 4636–4644.

29 I. L. Botto, A. C. Garcia and H. J. Thomas, *J. Phys. Chem. Solids*, 1992, **53**, 1075–1080.

30 M. Muñoz, C. I. Cabello, I. L. Botto, G. Minelli, M. Capron, C. Lamonier and E. Payen, *J. Mol. Struct.*, 2007, **841**, 96–103.

31 P. A. Nikulshin, N. N. Tomina, A. A. Pimerzin, A. Y. Stakheev, I. S. Mashkovsky and V. M. Kogan, *Appl. Catal., A*, 2011, **393**, 146–152.

32 *NIST Chemistry WebBook, NIST Standard Reference Database Number 69*, ed. P. J. Linstrom and W. G. Mallard, National Institute of Standards and Technology, Gaithersburg, MD, 20899, http://webbook.nist.gov, (retrieved July 14, 2014).

33 R. M. Silverstein and F. X. Webster, Infrared Spectrometry, in *Spectrometric Identification of Organic Compounds*, John Wiley & Sons, New York, 6th edn, 1998, pp. 71–143.

34 Q. Chen, D. P. Goshorn, C. P. Scholes, X. L. Tan and J. Zubieta, *J. Am. Chem. Soc.*, 1992, **114**, 4667–4681.

35 See ESI† for further discussion.